AIAA JOURNAL
Vol. 50, No. 12, December 2012

Technical Notes

Effect of Door Configuration on Cavity Flow Modulation Process

Nathan E. Murray* and Bernard J. Jansen†
University of Mississippi, University, Mississippi 38677

DOI: 10.2514/1.J051650

I. Introduction

WHEN fluid flowing over a bounding surface encounters a recess of significant size relative to the boundary layer, a complex three-dimensional (3-D) flow is established inside the recess that couples to the external flow in such a way that fluid-acoustic resonance can occur resulting in high-amplitude acoustic noise production, significant drag force increases, and high-amplitude hydrodynamic loading of the inclusive airframe. Research into these "cavity flows" dates back to over a half of a century to the seminal work of Rossiter [1] who proposed an empirical relationship for the prediction of resonant tones. For the interested reader, there are a number of excellent reviews [2–4].

In the current work, supersonic flow over a high-aspect-ratio cavity was studied with variations on the configuration of cavity doors: 1) no doors (baseline cavity), 2) doors open and protruding into the flow normal to the cavity opening, and 3) one door open with one door closed. These configurations are of current interest as modern high-speed aircraft are employing relatively long, shallow bays for carrying weapons.

The presence of payload bay doors adds to the complexity of the 3-D flowfield in and around a cavity. Wood et al. [5] references the flow visualization studies [6] (colored water surface flow) and [7] (vapor-screen photography) that show the vortical flow around finite width cavities at supersonic speeds both with and without doors. For a basic rectangular recess, counter-rotating, streamwise vortices stretch along the side of the cavity opening as illustrated in Fig. 1 (left). When doors are present, the vortices persist along the edges of the doors resulting in a vertical displacement between the vortices and the cavity opening (Fig. 1, right). This results in a change in the impingement of the shear layer on the trailing edge of the bay that in turn modifies the fluid/acoustic feedback process.

Here, the specific effect of the door configuration on the "efficiency" of the fluid/acoustic coupling is examined by evaluating Rossiter's phase lag constant, γ, using an amplitude modulation process approach. The interpretation of the cavity flow as an amplitude modulation process following the approach of [8,9] is presented in Sec. II. The cavity model, instrumentation, and flow conditions are described in Sec. III. The general spectral and spatial characteristics of the wall-pressure dynamics are presented in Sec. IV. Finally, Delprat's modulation process approach [8] is applied to the pressure spectra in Sec. V to evaluate the effect of the door configuration on the empirical constant γ. The results provide insight into the effect that the doors have on the cavity flow process as a whole.

Presented at the 17th AIAA/CEAS Aeroacoustics Conference, Portland, OR, June 6–8, 2011; received 12 October 2011; revision received 9 March 2012; accepted for publication 24 March 2012.

*Research Scientist II, Jamie L. Whitten National Center for Physical Acoustics. Senior Member AIAA.

†Senior R&D Engineer, Jamie L. Whitten National Center for Physical Acoustics. Member AIAA.

II. Cavity Flow as an Amplitude Modulation Process

Using a signal analysis approach [8,9] it is suggested that fluid-acoustic resonance induced by flow over a cavity is best described as a process that includes nonlinear distortion and amplitude modulation. This approach, which is conceptually supported [10–13], is quite powerful in describing 1) relationships between tonal peaks in the pressure spectra (Rossiter modes), 2) the presence of low-frequency components in the process, and 3) the cause for often observed time-depending switching between dominant modes observed [14,15]. Figure 2 illustrates the modulation process by showing the time trace for the first three Rossiter modes from a typical cavity flow wall pressure.

The basic form of Rossiter's empirical relationship to predict frequencies of cavity resonance is [1]

$$f_n = \frac{U_\infty}{L}\frac{n-\gamma}{M+1/\kappa} \tag{1}$$

where M is the Mach number, U_∞ is the freestream velocity, L is the cavity length, κ is the shear-layer convection velocity ratio to the freestream velocity, and γ is an empirically determined constant. Modifications to Eq. (1) have successfully improved the estimation of f_n in certain cases, such as high Mach number [16]. Here, Rossiter's original form is used for its broad applicability. Historically, it is interesting that the "standard" has been to adopt $\kappa = 0.57$ and $\gamma = 0.25$ while Rossiter's original work [1] listed γ values ranging from 0.25 to 0.58. In the years since Rossiter's seminal work, a number of researchers have concluded that the convection velocity ratio, $\kappa = 0.57$, is a very good estimate [17–19] leaving γ as the primary unknown.

To provide a physical concept for the constant γ, Rossiter [1] suggested the model shown in Fig. 3 in which γ is the vorticity wavelength fraction, which has passed by the bay at the instant when an acoustic wave is emitted from the aft wall. Using the illustration, Rossiter suggested that γ can be determined from the vortex spacing, λ_v, vortex convection speed, c_v, acoustic convection speed, c_a, and cavity length, L, as

$$\gamma\lambda_v = 2\lambda_v - L\frac{c_v}{c_a} - L \tag{2}$$

Subsequently, Rossiter demonstrated the agreement between Eqs. (1) and (2) algebraically, thereby validating the empirical relationship with the conceptual model. In this way, γ is seen as a phase lag parameter. Several authors have approached the problem in this way by specifically addressing the edge scattering process that occurs as the shear layer impinges on the aft wall [10,11,13,20,21].

In contrast, [8] suggests that γ represents a frequency ratio between the low-frequency, f_b, of the amplitude modulation and the "fundamental aeroacoustic loop frequency," f_a. This fundamental frequency can be determined from the interval between two "Rossiter" mode frequencies:

$$f_a = f_{n+1} - f_n = \frac{U_\infty}{L}\frac{1}{M+1/\kappa} \tag{3}$$

Comparing (3) to (1) yields

$$f_n = (n-\gamma)f_a \qquad \{n \geq 1, \gamma < 1\} \tag{4}$$

or,

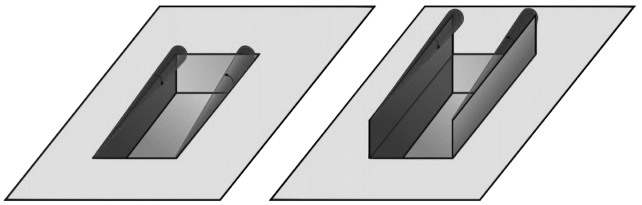

Fig. 1 Illustration of the effect of cavity doors on the streamwise vorticity location relative to the cavity openning: no doors (left), and doors open (right).

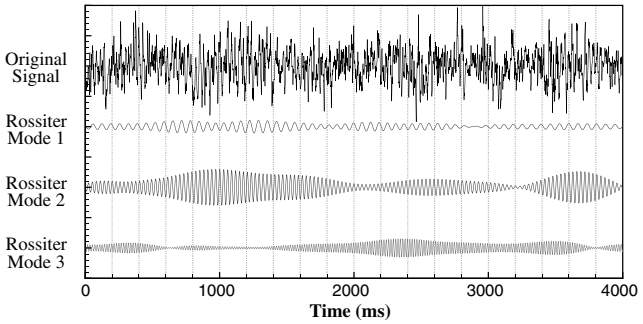

Fig. 2 Characteristic time traces of a Mach 0.6, $L/D = 6$ cavity pressure signal. Signals for the first three Rossiter modes were obtained by applying a narrow bandpass filter to the original signal [15].

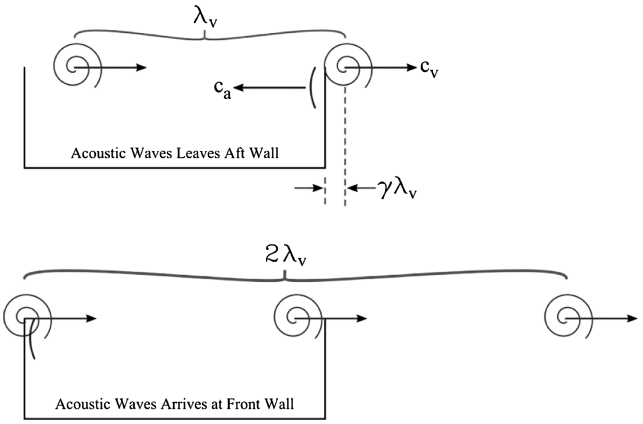

Fig. 3 Illustration of the physical model used by Rossiter to clarify his empirical relationship.

$$f_n = (nf_a - f_b) \tag{5}$$

Comparing Eqs. (4) and (5) gives γ as the frequency ratio, $f_b = \gamma f_a$, as proposed. Applying the approach to the experimental data requires taking the average of the frequency interval between pairs of spectral peaks resulting in γ being computed as

$$\gamma = (f_b)_{\text{mean}}/(f_a)_{\text{mean}} \tag{6}$$

This approach has recently been applied to subsonic cavity flows within the Mach number range of 0.2–0.65 [22], and it was found that γ asymptotically decreased from $\approx$0.2 to just less than 0.1 over their Mach number range.

Unlike Rossiter's empirical formula, Delprat's method [8] is not predictive. However, the application of Rossiter's formula has always been hampered by the unknown configuration and flow effects on the empirical constant, γ. Delprat's method now provides a concise method for evaluating these effects on γ to gain better insight into the cavity flow process.

III. Experimental Setup

A. Facility Description

All experimental data discussed herein were acquired in the 12 in. Tri-Sonic Wind Tunnel facility (TSWT) at the National Center for Physical Acoustics (NCPA) on The University of Mississippi campus. This facility, brought online in 2006, can be operated throughout the Mach number range from 0.3 to 1.0 and at supersonic Mach numbers of 1.5, 2.0, 3.5, and 5.0 using fixed geometry nozzle blocks. Test models can be positioned in either of two testing stations as shown in Fig. 4: the upstream location located in the Mach cone of the nozzle cart; and the supersonic test section (SSTS), which is located at the exit of the nozzle section. The SSTS has a fixed inlet cross section of 0.3×0.3 m, and its floor and ceiling can be diverged up to 0.635 cm over its 0.6 m length. Large windows can be installed in any or all of the SSTS side walls allowing full optical access to test models as needed. For the current experiments, the cavity model was installed in the ceiling of the SSTS with windows installed on the other three walls.

The TSWT is operated as a blowdown facility with closed loop control of the test section total pressure. The air supply comes from a high-volume centrifugal compressor system, which charges two 85 m^3 supply tanks to a maximum pressure of 41 atm. The supply tanks incorporate a thermal mass to aid in stabilizing the temperature drop during a test run. The high-volume compressor system incorporates two Ingersoll–Rand Centac compressors, which allows for rapid recharging of the supply air. The low-pressure unit provides air at 8.5 atm to a desiccant dryer that lowers the dew point to -51°C. The air is then pressurized further to 41 atm and stored in the supply tanks. The compressor system is isolated from the supply tanks prior to each run. With typical run times on the order of 15 to 30 s, it is possible to perform more than 10 test runs per hour on a continuous basis. As a result, the overall testing time is typically dictated by model changes rather than by supply charging.

B. Cavity Bay Model and Instrumentation

The rectangular cavity used for this study had a length of 22.86 cm and a depth of 2.54 cm giving an aspect ratio of $L/D = 9$. The cavity width was 5.08 cm. Flat panels were attached to the longitudinal edges of the cavity opening to represent doors. In the open position, the panels protruded into the oncoming flow to a height of one-half of

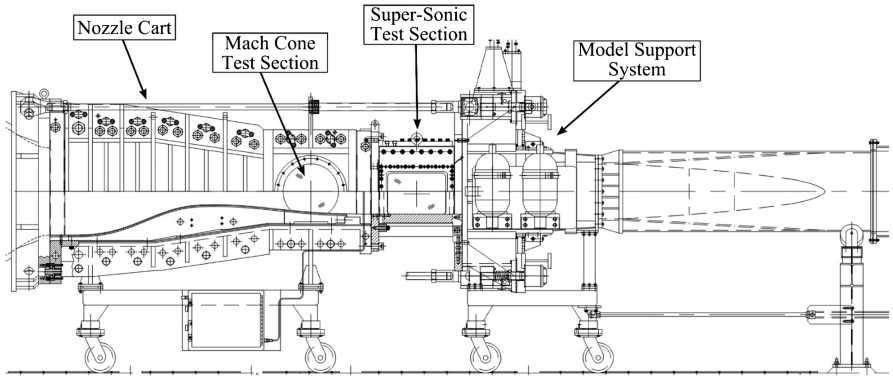

Fig. 4 Nozzle cart, test section, and model support system components of the NCPA TSWT facility.

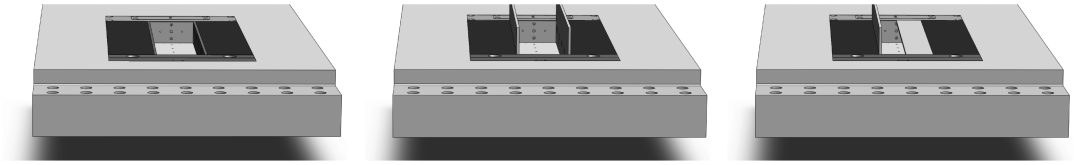

a) Baseline – No doors (N-N) b) Doors open (O-O) c) One door open (O-C)

Fig. 5 Illustration of the three door configurations examined.

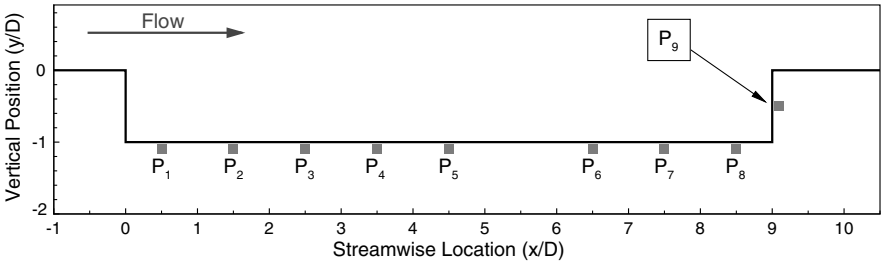

Fig. 6 Illustration of the location of the nine pressure transducers mounted along the cavity centerline.

the cavity width, or 2.54 cm. Three door configurations were tested as shown in Fig. 5: 1) no doors, which is a typical rectangular recess in a flat plane; 2) both doors open; and 3) only one door open. In the analysis to follow, these are referred to as no doors (N-N), both doors open (O-O), and only one door open (O-C), respectively.

Test runs were completed at a freestream Mach number of 1.5 with a total pressure of $P_0 \approx 206.8$ kPa. This resulted in a freestream dynamic pressure $Q = \frac{1}{2}\gamma P_s M^2 = 88.3$ kPa where P_s is the static pressure in the test section. The specific run conditions for each configuration are listed in Table 1. The boundary layer thickness, δ, at the leading edge of the cavity was estimated from schlieren images to be on the order of 1.14 cm suggesting $\delta/D = 0.45$.

Surface pressure signals were measured at nine locations along the centerline of the cavity: eight along the floor and one on the aft wall as shown in Fig. 6. Kulite model XCS-093-25SG transducers were used to measure the wall pressures. In each case, the signals were digitized at 100 kHz sample rate with a low-pass antialiasing filter set to 40 kHz. A total of 256×4096 samples were recorded for each configuration.

IV. Spectral and Spatial Characteristics of the Pressure Signals

Spectral analysis of the surface pressure signals show significant changes in the aeroacoustics for the three door configurations tested. With the pressure signals from the $k = 9$ transducers denoted as $P_k(t)$, the one-sided autospectral density was calculated as

$$G_{pp}(f) = \langle \hat{P}_k^{\star}(f)\hat{P}_k(f) \rangle \tag{7}$$

where $\hat{P}_k(f) = \mathcal{F}(P_k(t))$ denotes the 4096-point fast Fourier transform of the pressure signal, $\langle \cdot \rangle$ denotes ensemble averaging over the 256 blocks, and $(\cdot)^*$ denotes the complex conjugate. Figure 7 shows the spectra at the aft wall, a), and at two locations along the cavity floor, b) and c). First, the spectra are highly dependent on the spatial location of the sensor for this relatively long cavity. Second, the O-O configuration does not exhibit the typical spectral peaks related to Rossiter type behavior, rather, there are only broad humps in the O-O spectra and then only at select spatial locations. Also, the N-N and O-C configurations do show signs of fluid/acoustic type resonance. However, for the O-C configuration, the spectral peaks are shifted to a higher frequency and the peak amplitudes are larger relative to the broadband level. Finally, the door configuration's effect on the broadband levels is spatially dependent: compared to N-N, the broadband levels for O-C are lower for the aft wall but higher in the upstream end of the cavity at P_3.

Figure 8 shows the spatial distribution of the pressure dynamics by plotting the surface pressure spectra for each sensor at its corresponding location relative to the cavity length. The resulting contour surface shows the dominant resonant tones for the N-N and O-C configurations at their respective frequencies, but in this view, the spatial distribution of the dynamics at these frequencies is also evident. For example, the O-C configuration in Fig. 8c exhibits varying numbers of peaks in the streamwise (x/L) direction for each of the dominant tonal frequencies: the mode 2 tone at 1000 Hz has two peaks in the streamwise direction while the mode 3 tone at 1600 Hz has three peaks in the x/L direction.

There are other interesting features that appear in the surface-contour plots in Fig. 8. It is clear that the presence of the doors has a significant impact on the spectra. In fact, with both doors open (configuration O-O), there are no resonant tones anywhere in the cavity. However, at the lower frequencies, there is a clear dip in the amplitudes in the middle portion of the cavity length. In contrast, when one of the doors is closed (configuration O-C), the resonant tones are clearly dominant throughout the cavity, even at the upstream end. The O-C configuration also results in a broad low-frequency hump near 250 Hz (see Fig. 7b) that is not present for the N-N case.

V. Effect of Cavity Door Configuration

The shift in the spectral peak frequencies shows that the fluid-acoustic feedback is modified by the door configuration; this is not unexpected. However, a model for the modification of the feedback is not yet known. To move toward a better understanding of the effect that doors have on the feedback, the simple empirical model of Rossiter is revisited using the recent amplitude modulation approach of Delprat that was discussed in Sec. II.

Table 1 Tunnel run conditions for the three cavity configurations: O-O, both doors open; N-N, no doors; O-C, one door open and one door closed

Run No.	P_0 (kPa)	T_0 (°C)	P_s (kPa)	Q (kPa)	Mach	Configuration
874	205.5	21.7	55.8	88.3	1.5	O-O
878	205.5	20.6	55.8	88.3	1.5	N-N
879	206.2	21.5	55.8	88.3	1.5	O-C

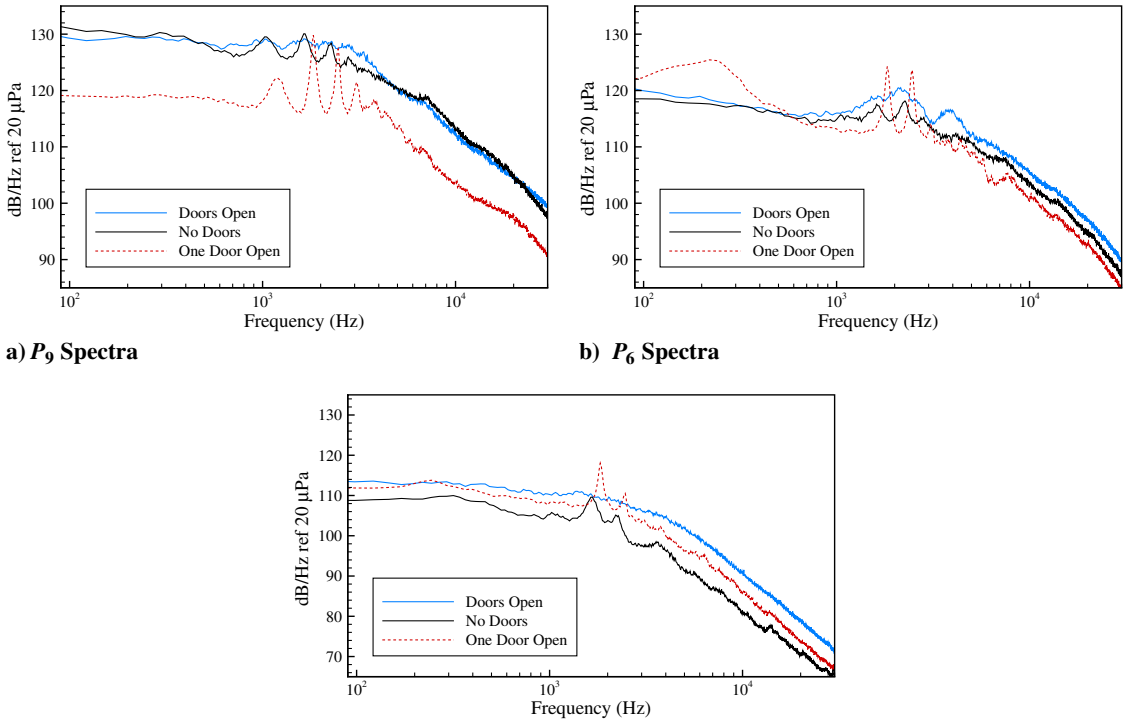

Fig. 7 Wall-pressure spectra for three locations showing the effect of the door configuration on the dynamic pressure in the cavity.

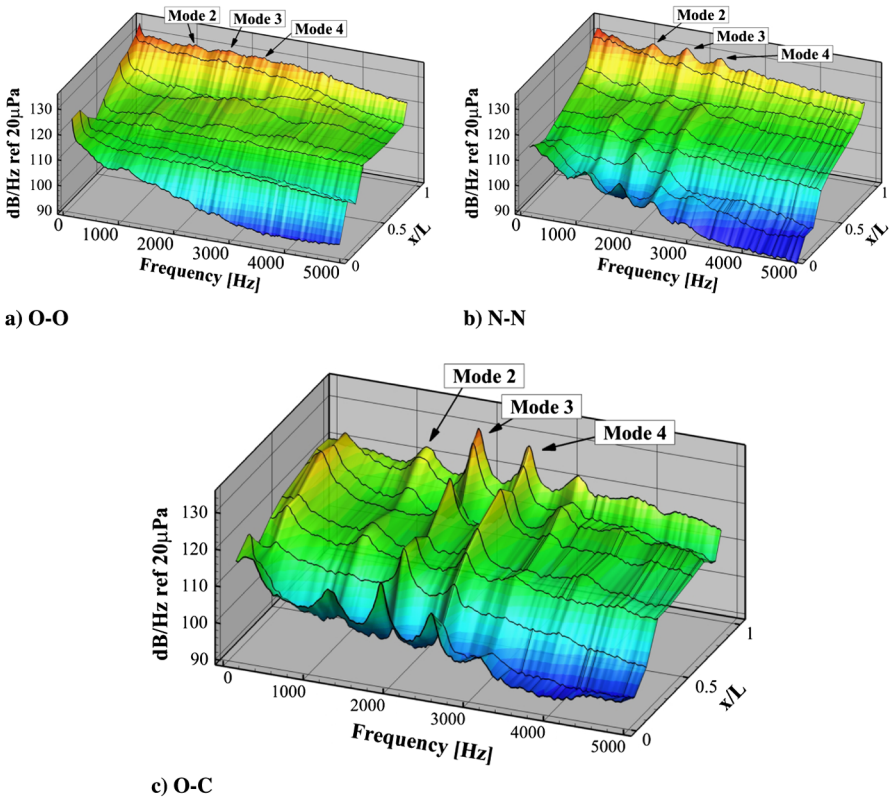

Fig. 8 Surface pressure spectra as a function of frequency and streamwise location for the three door configurations: no doors (N-N), doors open (O-O), and one door open (O-C).

A. Application of Modulation Model to Current Data

The first step in applying Delprat's method is to determine the frequencies of the spectral peaks. An automated method of determining the spectral peaks was demonstrated [22], which is useful for larger data sets. Here the spectral peaks were manually determined for the N-N and O-C configurations using Fig. 7a. The peak frequencies for modes 2 through 5 are listed in Table 2. Given the sampling rate (100 kHz) and the FFT length (4096 points), the frequency resolution in the narrowband spectra is $\Delta_f = 24.4$ Hz. The uncertainty in f_n is then taken to be $\mathcal{U}_{f_n} = \Delta_f/2 = 12.2$ Hz.

Table 2 Spectral peaks from Fig. 7a, resulting mean fundamental aeroacoustic loop frequency, $(f_a)_{\text{mean}}$, and convection speed ratio, κ

	Configuration N-N		Configuration O-C	
n	f_n	$f_{n+1} - f_n$	f_n	$f_{n+1} - f_n$
2	1041	609	1195	647
3	1650[a]	600	1842[a]	619
4	2250	554	2461	627
5	2804		3088	
$(f_a)_{\text{mean}}$	588 ± 7 Hz		631 ± 7 Hz	
κ	0.576 ± 0.025		0.660 ± 0.030	

[a]Denotes dominant tone

Table 3 Computation of the average fundamental modulation frequency $(f_b)_{\text{mean}}$ and the resulting ratio, γ, with the aeroacoustic loop frequency

	Configuration N-N			Configuration O-C		
n	f_n	$n(f_a)_{\text{mean}}$	$f_{b,n}$	f_n	$n(f_a)_{\text{mean}}$	$f_{b,n}$
2	1041	1176	135	1195	1262	67
3	1650	1764	114	1842	1893	51
4	2250	2352	102	2461	2524	63
5	2804	2940	136	3088	3155	67
	$(f_b)_{\text{mean}}$		122 ± 7.2			62 ± 7.2
	γ		0.21 ± 0.015			0.1 ± 0.015

Table 2 also lists the estimate for the fundamental aeroacoustic loop frequency, f_a, which was found to be 588 Hz for the N-N configuration and 631 Hz for the O-C configuration. The uncertainty in f_a was found to be $\mathcal{U}_{f_a} = \mathcal{U}_{f_n}/\sqrt{3} = \pm 7$ Hz given that only three values were used in the mean.

Assuming that M and U_∞ in Eq. (3) are constant, the convection ratio κ can be determined from f_a. For the current configuration, the cavity length is $L = 0.2286 \pm 0.001$ m. The measured test conditions (see Table 1) were $M = 1.5 \pm 0.025$ and $T_s = 203 \pm 0.6$ K. The acoustic speed based on the static temperature in the tunnel is $c_a = 285$ m/s giving a calculated freestream velocity of $U_\infty = 428 \pm 7$ m/s. Using these in Eq. (3), the convection speed ratio was computed as $\kappa = 0.576 \pm 0.025$ for the N-N configuration and $\kappa = 0.660 \pm 0.030$ for the the O-C configuration. The uncertainty estimates for κ were computed by evaluating the sensitivity of κ to the uncertainties of the other variables in Eq. (3). These uncertainty estimates are small compared to the increase in the magnitude of κ between configurations. This suggests that the presence of the closed door effectively increased the shear layer convection speed ratio.

To estimate the fundamental low-frequency of the modulation process, Eq. (5) is rearranged to solve for f_b with $f_a = (f_a)_{\text{mean}}$ from Table 2:

$$f_{b,n} = n(f_a)_{\text{mean}} - f_n \tag{8}$$

Therefore, for each spectral peak n, an estimate of the modulation frequency is obtained. Table 3 shows the results of this computation. The overall estimation of the modulation frequency is then the average of each $f_{b,n}$. Table 3 shows that $(f_b)_{\text{mean}} = 122$ Hz for configuration N-N and 62 Hz for configuration O-C with uncertainty estimates of ± 7.2 Hz. Using Eq. (6), the frequency ratio (as Delprat defines it) is $\gamma = 0.21$ for configuration N-N and 0.10 for configuration O-C with uncertainty estimates of $\mathcal{U}_\gamma = \pm 0.015$.

B. Summary of Door Configuration Effect

In summary, the application of Delprat's method to the current data results in $\kappa = 0.57$ and $\gamma = 0.21$ for the N-N configuration, whereas for the O-C configuration it is found that $\kappa = 0.660$ and $\gamma = 0.1$ (Table 4). Using these values in Eq. (1) results in the estimates for the spectral peaks that match the current spectral data to within the resolution of the spectra ($\pm \Delta_f = 24.4$ Hz).

Table 4 List of modulation frequencies and empirical constants computed using the method of [8]

Configuration	f_a (Hz)	f_b (Hz)	κ	γ
N-N	588 ± 7	122 ± 7.2	0.576 ± 0.025	0.21 ± 0.015
O-C	631 ± 7	62 ± 7.2	0.660 ± 0.030	0.1 ± 0.015

The modification of κ and γ by the door configuration suggests that the presence of a longitudinal edge covering a lateral opening below it has both increased the shear layer convection velocity and decreased the "phase-lag" in a Rossiter model sense. Granting that finite width cavities exhibit strong three-dimensionality, it still seems relevant to interpret γ in a phase-lag sense as suggested by Fig. 3. This is due to the fact that 1) cavity shear layers possess discrete coherent structures that regularly impinge on the trailing edge, 2) the impingement operates through some method to generate an acoustic wave [23–25], and 3) the acoustic wave emission can occur over a range of times due to the finite size of the coherent structure [26]. Although Delprat's method is suitable for computing γ as a frequency ratio, variations in γ suggest significant flow modifications that were responsible for altering the frequencies of the cavity flow process. In the present case, this approach suggests that the longitudinal edge of the closed door allowed the shear layer impingement to more efficiently generate acoustic disturbances (in the sense that the phase lag was reduced). This conclusion is plausible for two reasons: 1) it is known that a lateral edge protruding upstream from the aft wall would lead to the generation of "edge tones" very efficiently [20,25,27,28], and 2) the closed half of the cavity provides a sheltered path for acoustic waves to propagate upstream, which should enhance the acoustic feedback path.

VI. Conclusions

The effect of the door configuration on the aeroacoustics of supersonic flow past a cavity was examined using the amplitude modulation approach of Delprat. Three door configurations were tested: no doors (N-N), both doors open (O-O), and one door open with one door closed (O-C). With both doors open and protruding into the flow normal to the cavity opening, no resonant tones were observed in the pressure spectra measured on either the cavity floor or aft wall. Compared to N-N, the O-C configuration resulted in the resonant spectral tones that were sharper (narrower), higher in amplitude, and shifted to slightly higher frequency.

The resonant tones for the N-N and O-C configurations were examined by following the amplitude modulation approach of Delprat. The results indicated that the O-C configuration resulted in a higher fundamental aeroacoustic loop frequency, f_a, and a lower modulation frequency, f_b. Using these results to compute the shear layer convection ratio κ suggested that the closed door effectively increased the shear layer convection speed. Compared to the baseline (N-N), the O-C configuration resulted in a lower γ, which is interpreted by Delprat as the frequency ratio, $\gamma = f_b/f_a$. However, following Rossiter and interpreting γ as a phase lag suggests that the closed door increased the efficiency of the fluid/acoustic coupling in the sense that the phase lag decreased.

Acknowledgments

Funding was provided by a donation from Northrop Grumman Corporation. Special thanks to Praveen Panickar, Matthew Joachim, and David Rich for help with the data collection.

References

[1] Rossiter, J., "Wind-Tunnel Experiments on the Flow Over Rectangular Cavities at Subsonic and Transonic Speeds," Aeronautical Research Council, Rept. and Memoranda 3438, Ministry of Aviation, London, Oct. 1964.

[2] Rockwell, D., and Naudascher, E., "Review—Self-Sustaining Oscillations of Flow Past Cavitites," *Journal of Fluids Engineering*, Vol. 100, No. 2, 1978, pp. 152–165. doi:10.1115/1.3448624

[3] Cattafesta, L., Williams, D., Rowley, C., and Alvi, F., "Review of Active Control of Flow-Induced Cavity Resonance," *33rd AIAA Fluid Dynamics Conference*, AIAA Paper 2003-3567, June 2003.

[4] Rowley, C., and Williams, D., "Dynamics and Control of High-Reynolds-Number Flow Over Open Cavities," *Annual Review of Fluid Mechanics*, Vol. 38, Jan. 2006, pp. 251–276. doi:10.1146/annurev.fluid.38.050304.092057

[5] Wood, R. M., Wilcox, F. J., Bauer, S. X. S., and Allen, J. M., "Vortex Flows at Supersonic Speeds," NASA Langley Research Center, TP-2003-211950, Hampton, VA, March 2003.

[6] Wilcox, F., Jr., "Use of a Colored Water Flow Visualization Technique in a Supersonic Wind Tunnel to Investigate Cavity Flow Fields," *Flow Visualization VI—Proceedings of the Sixth International Symposium on Flow Visualization*, Yokohama, Japan, Springer–Verlag, Germany, Oct. 1992, pp. 41–45.

[7] Stallings, R. L., Jr., Wilcox, F. J., Jr., and Forrest, D. K., "Measurements of Forces, Moments, and Pressures on a Generic Store Separating From a Box Cavity at Supersonic Speeds," NASA TP-3110, 1991.

[8] Delprat, N., "Rossiter's Formula: A Simple Spectral Model for a Complex Amplitude Modulation Process?," *Physics of Fluids*, Vol. 18, No. 7, 2006, pp. 71, 703–4. doi:10.1063/1.2219767

[9] Delprat, N., "Low-Frequency Components and Modulation Processes in Compressible Cavity Flows," *Journal of Sound and Vibration*, Vol. 329, No. 22, Oct. 2010, pp. 4797–4809. doi:10.1016/j.jsv.2010.05.013

[10] Bilanin, A., and Covert, E., "Estimation of Possible Excitation Frequencies for Shallow Rectangular Cavities," *AIAA Journal*, Vol. 11, No. 3, 1973, pp. 347–351. doi:10.2514/3.6747

[11] Tam, C., and Block, P., "On the Tones and Pressure Oscillations Induced by Flow Over Rectangular Cavities," *Journal of Fluid Mechanics*, Vol. 89, No. 2, 1978, pp. 373–399. doi:10.1017/S0022112078002657

[12] Knisely, C., and Rockwell, D., "Self-Sustained Low-Frequency Components in an Impinging Shear Layer," *Journal of Fluid Mechanics*, Vol. 116, 1982, pp. 157–186. doi:10.1017/S002211208200041X

[13] Kerschen, E., and Tumin, A., "A Theoretical Model of Cavity Acoustic Resonances Based on Edge Scattering Processes," *41st AIAA Aerospace Sciences Meeting and Exhibit*, AIAA Paper 2003-0175, Jan. 2003.

[14] Kegerise, M., Spina, E., Garg, S., and Cattafesta, L., "Mode-Switching and Nonlinear Effects in Compressible Flow Over a Cavity," *Physics of Fluids*, Vol. 16, No. 3, 2004, pp. 678–687. doi:10.1063/1.1643736

[15] Murray, N., "Flow Field Dynamics in Subsonic Cavity Flows," Ph.D. Thesis, Univ. of Mississippi, Oxford, MS, 2006.

[16] Heller, H., Holmes, D., and Covert, E., "Flow-Induced Pressure Oscillations in Shallow Cavitites," *Journal of Sound and Vibration*, Vol. 18, No. 4, 1971, pp. 545–553. doi:10.1016/0022-460X(71)90105-2

[17] Ahuja, K. K., and Mendoza, J., "Effects of Cavity Dimensions, Boundary Layer, and Temperature on Cavity Noise with Emphasis on Benchmark Data to Validate Compuational Aeroacoustic Codes," NASA CR-4653, April 1995.

[18] Larchevêque, L., Sagaut, P., Le, T., and Comte, P., "Large-eddy Simulation of a Compressible Flow in a Three-dimensional Open Cavity at High Reynolds Number," *Journal of Fluid Mechanics*, Vol. 516, Oct. 2004, pp. 265–301. doi:10.1017/S0022112004000709

[19] Murray, N., and Ukeiley, L., "Wall-Pressure Modes in Subsonic Cavity Flows," *11th AIAA/CEAS Aeroacoustics Conference*, AIAA Paper 2005-2801, May 2005.

[20] Powell, A., "On the Edgetone," *Journal of the Acoustical Society of America*, Vol. 33, No. 4, 1961, pp. 395–409. doi:10.1121/1.1908677

[21] Rowley, C., Colonius, T., and Basu, A., "On Self-Sustained Oscillations in Two-Dimensional Compressible Flow Over Rectangular Cavities," *Journal of Fluid Mechanics*, Vol. 455, 2002, pp. 315–346. doi:10.1017/S0022112001007534

[22] Malone, J., Debiasi, M., Little, J., and Samimy, M., "Analysis of the Spectral Relationships of Cavity Tones in Subsonic Resonant Cavity Flows," *Physics of Fluids*, Vol. 21, No. 5, 2009, p. 055103-9. doi:10.1063/1.3139270

[23] Rockwell, D., and Knisely, C., "The Organized Nature of Flow Impingement Upon a Corner," *Journal of Fluid Mechanics*, Vol. 93, No. 03, 1979, pp. 413–432. doi:10.1017/S0022112079002573

[24] Rockwell, D., and Naudascher, E., "Self-Sustained Oscillations of Impinging Free Shear Layers," *Annual Review of Fluid Mechanics*, Vol. 11, Jan. 1979, pp. 67–94. doi:10.1146/annurev.fl.11.010179.000435

[25] Rockwell, D., and Knisely, C., "Vortex-Edge Interaction: Mechanisms for Generating Low Frequency Components," *Physics of Fluids*, Vol. 23, No. 2, 1980, pp. 239–240. doi:10.1063/1.862962

[26] Murray, N., and Ukeiley, L., "Modified Quadratic Stochastic Estimation of Resonating Subsonic Cavity Flow," *Journal of Turbulence*, Vol. 8, 2007, pp. N53. doi:10.1080/14685240701656121

[27] Howe, M., "Edge, Cavity and Aperture Tones at Very Low Mach Numbers," *Journal of Fluid Mechanics*, Vol. 330, 1997, pp. 67–84. doi:10.1017/S0022112096003606

[28] Panaras, A. G., "Pressure Pulses Generated by the Interaction of a Discrete Vortex With an Edge," *Journal of Fluid Mechanics*, Vol. 154, 1985, pp. 445–461. doi:10.1017/S0022112085001616

M. Glauser
Associate Editor